PAPER • OPEN ACCESS

Influence of imperfections on dynamic properties of oscillating rod

To cite this article: V Dekys *et al* 2020 *IOP Conf. Ser.: Mater. Sci. Eng.* **776** 012068

View the article online for updates and enhancements.

Influence of imperfections on dynamic properties of oscillating rod

V Dekys[1], P Novak[1], D Milosavljevic[2], M Nekoranec[1] and O Stalmach[1]

[1] University of Zilina, Faculty of Mechanical Engineering, Univerzitna 1, 01026 Žilina, Slovak Republic
[2] Faculty of Mechanical Engineering, University of Kragujevac, Sestre Janjic 6, 34000 Kragujevac, Serbia

E-mail: vladimir.dekys@fstroj.uniza.sk

Abstract. The paper deals with the analysis of the influence of boundary conditions on the dynamic properties of a mechanical system. The steel bar is fixed in one place so that it is inserted under the hydraulic press. The pressure force in the press changes and models the imperfect fixation of the bar. The effect of bond imperfection is evaluated based on rod vibration analysis. This problem is solved computationally, by FEM and the results are compared with experimental measurement.

1. Introduction

Sometimes the problem is solved: The computational model was prepared and verified by experiment. This procedure can be understood to have verified the model's accuracy by experiment. The judge to determine the correctness of the calculation model is an experiment. The results of the experiment are considered critical in this procedure. However, another problem can be solved when we verify the results of the experiment with a computational model. This approach may lead to the notion that either the experiment or the calculation procedure becomes infallible in this assessment, or that one procedure is superior to the other. It is more correct to talk about the results obtained from the experiment and the model, because the experiment and the model may not be exactly the same in their assumptions and procedures and thus may not give the same values, even if these procedures are considered correct.

When solving dynamics tasks, more precisely vibrations, we often encounter that the calculated natural frequencies [1, 2] of the analyzed object are different from those determined by the experiment [3]. If the problem is boundary condition [4–8], then the explanation may be that in the computational model the boundary condition prevents any displacement and rotation until the condition is fully satisfied in the experimental model. Then, the computational model with such boundary conditions appears to be a model with a higher stiffness than the test object used in the experiment and the natural frequencies determined by the computation are higher.

Another reason may be that the real model will have very small but non-zero damping [9–10], while the computational model is often a non-damping model. On the other hand, the presence of damping reduces the natural frequency. Neglect of damping is often associated with ignorance of the damping value for the calculation model and also because of the required simplicity of the model.

The article will deal with the determination of the 1st resonance frequency (based on the experiment) and the 1st natural frequency for this rod (based on calculation) for a cantilever steel

beam. In the experiment, the beam was fixed at one end in a hydraulic manual press. The press simulated a different force in the fixed end and the first resonant frequency was determined for these forces [11–13]. Subsequently, a numerical model was created in the AnsysWorkbench, when different boundary conditions were simulated by different great forces in this fixed end. The first natural frequency was determined by computational modal analysis. The measured and calculated values of these frequencies were compared [14–18].

2. The experiment, determination of the first resonant frequency

The steel test beam of rectangular cross section 5 × 20 mm length 490 mm of material EN: S235JRG1, STN 11373 was used. A force sensor was placed on one end of the bar and the bar together with the sensor was placed on the frame of the hydraulic hand press. A hydraulic piston pressed the force sensor (figure 1). The beam so fastened was stimulated and its response of its unloaded part was measured.
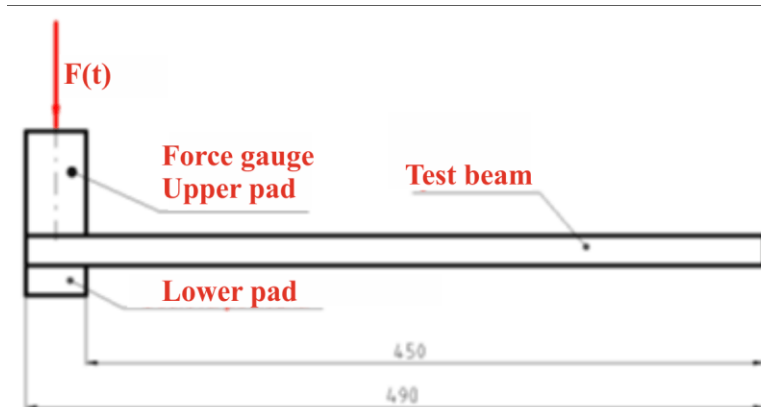
Figure 1. Experimental set-up, test rod - cantilever beam, force acting on fixed end.

Initially, the impulse hammer excitation used in experimental modal analysis was used. However, at low values of the pressure forces exerted by the hydraulic press, this excitation method was not suitable. If a higher force impact was performed, then the rod bearing was unstable, the test object was displaced and its unloaded length changed. This was the reason why this method of stimulation was rejected. It should be noted, however, that the use of a modal hammer will provide a pulsed force signal and classical experimental modal analysis tools may be used.

In practice, a bump test is used to estimate resonant frequencies. In this test, an impact of a suitable body on the test object is useful as stimulus. Impact is considered a pulse load (this input signal is not measured) and the resonance frequencies are estimated based on peaks in the output signal spectrum.

The beam was sufficiently stimulated even with a light impulse from the experimenter's finger. However, we considered this procedure to be very subjective and we did not use it for further measurements.

On the basis of measurements when looking for an excitation source, when the beam was stimulated by a pulse hammer and a finger, a resonance frequency was detected at around 20 Hz.

More significant vibration of the test object occurred also during the transfer of energy from the vibration source near the test object to this test object. A test stand for long-term fatigue tests was located around the test beam. This stand was a source of vibrations from which energy was transmitted to the frame of a hand press with a dominant peak at 25 Hz. This vibration source was capable to excite the beam and this fatigue capability was used in the tests. Let us specify that not only the 25 Hz harmonic component but also the harmonics were transferred to the press frame. The presence of harmonic components presents the occurrence of mechanical looseness on the fatigue test stand.

The F_{LOAD} fixed end force was measured with a DAKO S-60 strain gauge force sensor at range ±60 kN. The test device is shown in figure 2.

The response of the object to stimulation by the vibration source was measured by Polytec PDV100 laser vibrometer, i.e. the vibration velocity was measured. The cDAQ National Instrument measuring system with NI 9234 and NI USB 9237 modules located in chassis 9178 as well as SW LabVIEW, NI Signal Express was used to measure pressure force and vibration velocity.

Figure 2. Testing equipment: manual press, tested beam, force sensor, laser Doplervibrometer.

Because there was also a rare excitation of resonant frequencies in the range of 200–300 Hz and the source of the resonance unknown in this range, the measured signal was filtered by a narrow-pass filter in the range 15–21 Hz. To determine the resonant frequency, the filtered signal was input to the SW module of the THD calculation (Total Harmonic Distortion, it is measure the amplitudes of the harmonic system to the amplitude of the fundamental frequency), whose output parameter is also the fundamental frequency. This frequency is the first resonance frequency to be searched for f_{R1}. The sampling rate for measuring force and vibration speed was 1 kHz, the measurement time at the selected load level was 8 s.

The output of the experimental part was the relationship between the compressive force and the first resonant frequency in figure 3, Eq. (1):

$$f_{R1} = f(F_{LOAD}). \tag{1}$$

In figure 3 shows the resonance frequency values f_{R1} (red cross) for various pressure values. 430 data were used for processing. Regression dependence, Eq. (2), was determined for the following data and its parameters a, b and determination coefficient R^2 were also determined:

$$f_{R1} = a\,F_{LOAD}{}^{b} \tag{2}$$

$$a = 18.71, \quad b = 6.78 \cdot 10^{-3}, \quad R^2 = 0.958. \tag{3}$$

The prediction interval (95 %) for the dependence (2) is shown by the dashed line in figure 3. The uncertainty in the force measurement was ΔF = ±0.5 % and ±250 N respectively. Based on the high value of the coefficient of determination, the regression model (2, 3) was accepted.
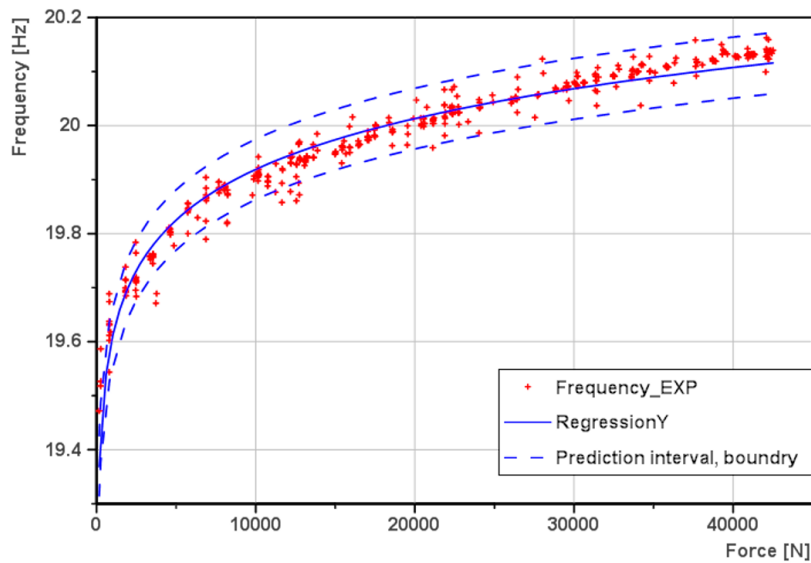
Figure 3. Experimental results, regression curve, boundary of prediction interval wit probability 0.95.

## 3. The FEM model, determination of the first natural frequency.

Solid 185 linear elements were used in the computational model. Boundary condition (fixed support) was applied to the bottom of the top pad and to the top of the bottom pad, translation:

$$u_x = u_z = 0, \quad u_y 0. \tag{4}$$

A contact between pads and beam (Contact Bodies / Target Bodies), type of contact "Rough" has been defined. The compressive force load was applied using the boundary condition "Bolt Pretension". Values E = 200 MPa (Young's modulus), density ρ = 7850 kg m^{-3} and free bar length l = 450 mm were input data for calculation, these data corresponded to material: steel STN 11 373 and EN S235JRG1 respectively. The input data were obtained from the rod manufacturer's technical specifications. However, it should be noted that these input data have a non-zero variance, which should be taken into account when comparing the results from the experiment and the computational model.

A model for computational analysis is shown in figure 4. The output of the calculation was the dependence of the first natural frequency f_{N1} on the force (Eq. (5)). This dependence will be presented and discussed in the next chapter.

$$f_{N1} = f(F_{LOAD}). \tag{5}$$
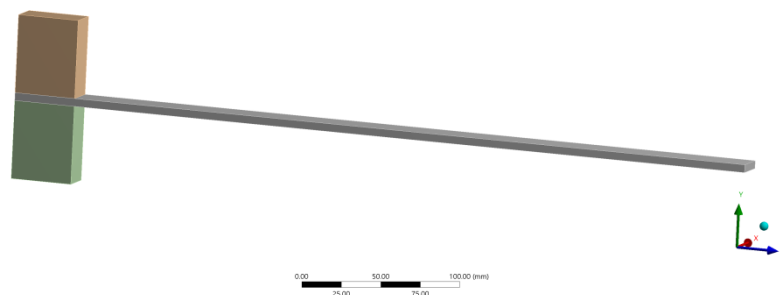
Figure 4. Computational model, upper brown block replaces upper pad and force sensor, lower green block replaces lower pad.
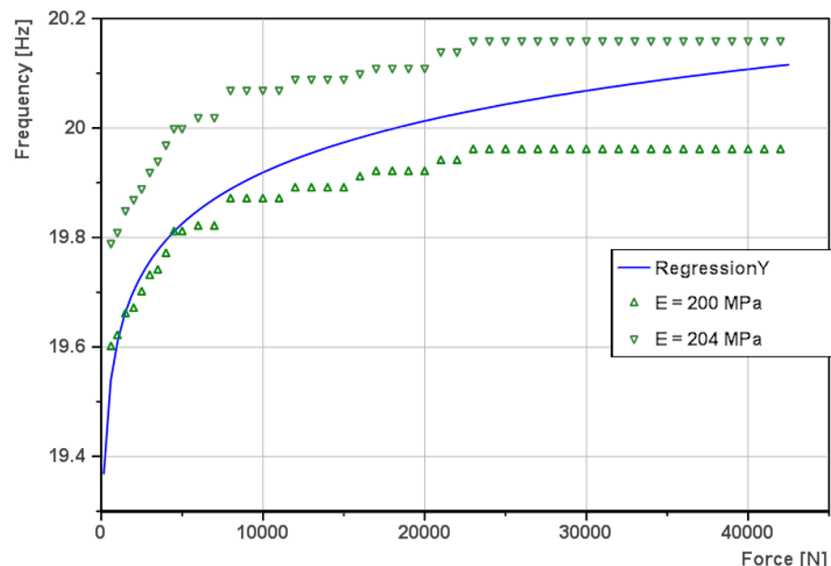
4. Comparison of results

In figure 5 shows a comparison of computational simulation results and experiment. The following conclusions for comparison and explanation were made.

The data from the experiment was replaced with f_{R1} by the regression dependence of "RegressionY" in figure 5. For input nominal data E = 200 MPa, l, and F_{LOAD} were determined by modal analysis f_{N1}.

Material data of the beam used was selected as nominal data from material sheets. The actual beam may have other parameters within the declared variance. Figure 5 also shows the dependence of the natural frequency on the load force for E = 204 MPa, which is 2 % higher than the nominal. The regression dependence is then limited and the boundaries of this region are the points or natural frequencies calculated for the nominal value of the Young's modulus and the modulus increased by 2 %.

Both dependencies are increasing but the regression dependence frequency increases faster for higher force values than the calculated frequency.

The calculated frequency-force dependencies were not replaced by the curve. The waveform is the result of solving a non-linear contact problem.


Figure 5. Comparison of regression dependence from experiment and FEM results for different values of Young's modulus.

The deviation f_{N1} for the given values of the modulus of elasticity E = 200 MPa and E = 204 MPa from f_{R1} is shown in figure 6. The deviation f_{N1} from f_{R1} does not exceed 1.3 %.

The deviation f_{N1} for the given values of the modulus of elasticity E = 200 MPa and E = 204 MPa from f_{R1} is shown in figure 6. The deviation f_{N1} from f_{R1} does not exceed 1.3 %. The bandwidth of the calculated frequencies that covers f_{N1} is approximately 1 %.

Similar calculations can be performed for changed values ρ and l. If $\Delta\rho$ = ±2.5 %, then Δf_{N1} = ±1.3 % and if Δl = ±10%, then Δf_{N1}= ±0.5 %. The band width for ΔE, $\Delta\rho$, Δl then reaches approximately ±3 % and this band covers the Δf_{R1} values determined by the experimenton. Possible changes in beam length were considered, because at low forces the rod could shift and the experimenter could not observe this.

On the basis of the above, it was concluded that the regression curve covered by the interval of calculated values and the authors of the article should be satisfied with the approximation found. However, the regression curve has a different slope (the first derivative) than the boundary curves and therefore we consider it necessary to consider the correction of the computational model.
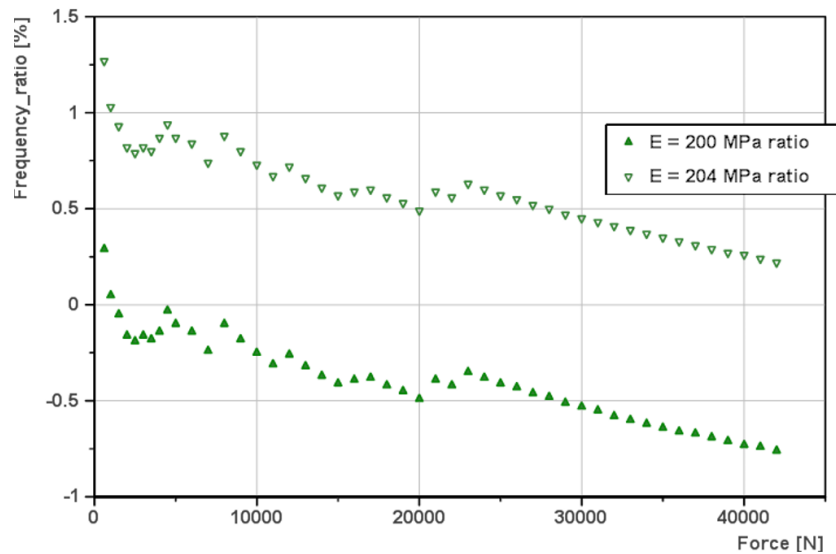
Figure 6. Comparing the deviation of the calculated frequency values for the different Young module values from the measured frequency value.

5. Conclusion

The paper presents a method of modeling the boundary condition of an oscillating rod in a vertical plane, when the real contact of the horizontal bar allows displacements in its contact in the horizontal direction. The appropriate FEM model was built. Within the analyzed tolerances in the input parameters, a very good agreement was reached between the computational model used and the experiment. The maximum deviation of the calculated natural frequencies from the experimentally determined resonant frequencies does not exceed 3 %.

However, it should be noted that the damping was neglected in the above calculation model. In addition, the slope of the regression curve used is different than the slope of the calculated natural frequencies on the force at impact. This fact should be further analysed.

Material input data were not verified by a separate experiment in the solution, but data corresponding to the used material standard were used. If the input parameters verified by a separate experiment were used, the percentage deviations could change. Therefore, consider the data presented in the article as an estimate using nominal input data.

6. References

[1]   Sapietova A, Petrech R and Petrovic M 2014 Analysis of the dynamical effects on housing of the axial piston hydromotor *Appl. Mech. Mater.* **474** 357–362
[2]   Sapietova A, Bukovan J, Sapieta M and Jakubovicova L 2017 Analysis and implementation of input load effects on an air compressor piston in MSC.ADAMS *Procedia Eng.* **177** 554–561
[3]   Trebuna F, Simcak F, Bocko J and Pastor M 2014 Complex approach to the vibrodiagnostic analysis of excessive Cross Mark vibration of the exhaust fan *Eng. Fail. Anal* **37** 86–95
[4]   Nad M, Duris R and Nanasi T 2018 Prediction of modal properties of circular disc with pre-stressed fields *MATEC Web Conf.* **157** 02034
[5]   Dudziak M, Domek G and Kołodziej A 2016 Variation of static parameters of cooperation in axisymmetric connection *Procedia Eng.* **136** 56–62
[6]   Nad M, Rolnik L and Cicmancova L 2017 Prediction of changes in modal properties of the Euler-Bernoulli beam structures due to the modification of its spatial properties *Int. J. Struct. Stab. Dy.* **17** 1740014
[7]   Milosavljevic D, Bogdanovic G, Veljovic L and Radakovic A 2015 Wave propagation in layer with two preferred directions *Int. J. Nonlin. Mech.* **73** 94–99

[8]   Radakovic A, Bogdanovic G, Milosavljevic D, Veljovic L and Cukanovic D 2017 Using high-order deformation theory in the analysis of Lamb's waves propagation in materials reinforced with two families of fibres *Acta Mech*. **228** 187–200

[9]   Segla S and Musil M 2018 Comparison of passive and semi-active horizontal platform suspensions *The. Vjesn*. **25** 1659–1666

[10]   Zapomel J, Ferfecki P and Kozanek J 2015 Modelling of magnetorheological squeeze film dampers for vibration suppression of rigid rotors *Int. J. Mech. Sci*. **127** 191–197

[11]   Zmindak M, Radziszewski L, Pelagic Z and Falat M 2015 Fem/bem techniques for modelling of local fields in contact mechanics *Communications - Scientific Letters of the University of Zilina* **173** 37–44

[12]   Soukup J, Klimenda F, Skočilas J and Žmindák M 2019 Finite element modelling of shock wave propagation over obstacles *Manufacturing Technology* **19** 499–507

[13]   Žmindak M 2018 Dynamic and sensitivity analysis general non-conservative asymmetric mechanical systems *Strojnícky casopis – Journal of Mechanical Engineering* **68** 105–124

[14]   Piekarska W, Sága M, Goszcynska-Kroliszewska D, Domanski T and Kopas P 2018 Application of analytical methods for determination of hardness distribution in welded joint made of S1100QL steel *MATEC Web Conf*. **157** 02041

[15]   Handrik M, Vaško M and Kopas P 2012 Parallel and distributed implementation of optimization algorithms in FE analyses *Sci. J. Sil. Univ. Technol. – Ser. Transp*. **76** 67–74

[16]   Saga M, Vasko M, Sagova Z and Handrik M 2018 Effective algorithm for structural optimization subjected to fatigue damage and random excitation *Sci. J. Sil. Univ. Technol. – Ser. Transp*. **99** 149–161

[17]   Saga M, Vasko M, Handrik M and Kopas P 2019 Contribution to random vibration numerical simulation and optimisation of nonlinear mechanical systems *Sci. J. Sil. Univ. Technol. – Ser. Transp*. **103** 143–154

[18]   Kovacikova P, Vavro J and Vavro J Jr 2018 Numerical modal analysis for vibration-damping properties of ductile cast *MATEC Web Conf*. **157** 02019